Residues in the Hydrophilic Face of Putative Helix 8 of Oxytocin Receptor Are Important for Receptor Function†

Miao Zhong, Amy M. Navratil, Colin Clay, and Barbara M. Sanborn*

Department of Biomedical Sciences, Colorado State University, Fort Collins, Colorado 80523

Received October 23, 2003; Revised Manuscript Received January 23, 2004

ABSTRACT: Oxytocin receptor (OTR) activates the GTP-binding protein $G\alpha_q$. To investigate whether the N-terminal region of the fourth intracellular domain of this receptor, which forms putative helix 8, plays a role in coupling, its hydrophilic residues (H7.59, H7.62, E7.63, Q7.66, and R7.67) were mutated individually to alanine. In COSM6 cells, these mutants were expressed at equivalent concentrations, but at lower concentrations than OTR. Alanine substitution for H7.62 or Q7.66 did not substantially affect the affinity for OT (K_d = 0.63 and 0.48 nM, respectively, vs 0.52 nM for the wild type), whereas substitution for H7.59, E7.63, or R7.67 reduced the affinity 5−6-fold. When expressed at equal concentrations, OTR-H7.62/A and OTR-Q7.66/A stimulated phosphatidylinositide turnover as well as OTR, whereas OTR-H7.59/A, OTR-E7.63/A, and OTR-R7.67/A exhibited an impaired ability to respond to OT. Therefore, residues H7.59, E7.63, and R7.67 within the putative hydrophilic interface appeared to influence both the OTR conformation and $G\alpha_q$ coupling. To explore this further, five multiple alanine substitution mutants were constructed. Alanine modification at H7.62 and Q7.66 did not substantially affect the affinity for OT (K_d = 0.75 nM), whereas any combination of alanine substitutions for H7.59, E7.63, and R7.67 produced mutant receptors that lost high-affinity ligand binding. While OTR-(H7.62,Q7.66)/A exhibited PLC activation equivalent to that of OTR, receptors with two or more changes in H7.59, E7.63, and R7.67 lost the ability to respond to OT in a dose-dependent manner. Five residues (L7.60, F7.61, L7.64, V7.65, and F7.68) in the opposite hydrophobic interface were also mutated to alanine. None of these substitutions affected ligand binding; only OTR-(L7.60,F7.61)/A had a somewhat weaker ability to activate PLC. These data are consistent with the prediction that these residues lie within an amphipathic α-helix and emphasize the importance of this hydrophilic interface, and particularly of H7.59, E7.63, and R7.67, in OTR function.

Oxytocin (OT) is a nonapeptide hormone that regulates the contractility of uterine smooth muscle at parturition and mammalian myoepithelium during lactation. The physiological effects of OT are mediated via activation of a number of intracellular events by a specific OT receptor (OTR)[1] of the rhodopsin-like or class A G-protein-coupled receptor (GPCR) family (*1*). The nature of the coupling and activation of class A GPCRs has been extensively explored. Structure−function studies have implicated the importance of cytoplasmic loops 2 and 3 and related juxtamembrane regions in receptor−G-protein interactions (*2*). The predominant change in the relative configurations of the transmembrane (TM) helices during activation of rhodopsin and other class A GPCRs is a rotation of helix 6 accompanied by its movement away from helix 3 (*3*−*6*) and, at its cytoplasmic side, toward helix 5 (*7*, *8*). TM helix 7 has also been proposed to participate in interhelical constraints to keep angiotensin II type 1A receptor (*9*), rhodopsin (*10*), and serotinin type 2C receptor (*11*) in the ground state and to undergo an orientation rearrangement following activation (*12*, *13*).

The C-terminal sequence following helix 7 has been shown in many receptors to contain important determinants for receptor internalization and desensitization (*14*). However, its specific role in G-protein coupling remains controversial, ranging from being essential (*15*) to being unnecessary (*16*, *17*). One of the most striking findings from the high-resolution X-ray crystal structure of bovine rhodopsin was the presence of helix 8 in its C-terminal region between the extension of helix 7 and the highly conserved cysteine pair (*18*). A similar α-helical structure was also observed in peptides corresponding to comparable sequences of both *β*-adrenergic receptor (*19*) and angiotensin II type 1A receptor (*20*).

OTR is known to couple primarily to $G\alpha_q$ (*21*, *22*), but coupling to $G\alpha_i$ (*23*) and $G\alpha_h$ (*24*) has also been reported. A truncated rat OTR mutant lacking the 39 carboxyl-terminal residues but including the sequence beyond the conserved cysteine pair functioned in a manner similar to that of wild-type OTR; deletion of 12 additional residues, including that cysteine pair, resulted in a mutant that was uncoupled from $G\alpha_q$-mediated pathways but was still able to activate pertussis toxin-sensitive calcium entry (*25*). The cysteine pair itself

† Supported in part by grants from the R. A. Welch Foundation and NIH Grant HD09618.

* To whom correspondence should be addressed: Department of Biomedical Sciences, 102 Physiology Box 1680, Colorado State University, Fort Collins, CO 80523. Phone: (970) 491-4263. Fax: (970) 491-7569. E-mail: Barbara.Sanborn@colostate.edu.

[1] Abbreviations: Con A, concanavalin A; FITC, fluorescein isothiocyanate; G-protein, heterotrimeric GTP-binding protein; GPCR, G-protein-coupled receptor; IP_3, inositol 1,4,5-triphosphate; OTR, oxytocin receptor; V_2R, vasopressin type 2 receptor; PLC, phospholipase C; TM, transmembrane; PI, phosphatidylinositide.

10.1021/bi035899m CCC: $27.50
Published on Web 03/04/2004

is not required for activity (*25*), but the 51-residue deletion would remove part of the putative helix 8 as well. Since α-helices are important determinants in protein−protein interactions, a helical structure in this C-terminal region of OTR may play an important role in this protein. We provide evidence that residues in this region that have significant consequences for OTR function are arranged in a pattern consistent with their location in a hydrophilic face of an amphipathic helix.

MATERIALS AND METHODS

Chemicals and Plasmids. [^{3}H]Myoinositol (22.3 Ci/mmol) and [tyrosyl-2,6-^{3}H]oxytocin (33 Ci/mmol) were obtained from DuPont-NEN Life Science Products (Boston, MA), and bovine serum albumin (BSA, fatty acid free, fraction V) was from ICN Biomedicals Inc. (Irvine, CA). Human oxytocin was obtained from Sigma Chemical Co. (St. Louis, MO). Alexa 594-conjugated concanavalin A (Con A) was obtained from Molecular Probes Inc. (Eugene, OR). The fluorescein isothiocyanate (FITC)-conjugated donkey anti-goat antibody and the antibodies directed against OTR and PKA catalytic subunit were obtained from Santa Cruz Biotechnology Inc. (Santa Cruz, CA). Cell culture reagents were obtained from Life Technologies Inc. (Gaithersburg, MD). The GeneEditor site-directed mutagenesis kit and Transfast transfection reagent were obtained from Promega (Madison, WI). AG 1-X8 resin was obtained from Bio-Rad Laboratories, Inc. (Hercules, CA), and nitrocellulose membranes were from Schleicher & Schuell (Keene, NH). MultiScreen filter plates (FB) were purchased from Millipore (Bedford, MA).

The cDNA clone of human OTR was obtained from M. J. Brownstein (National Institutes of Health, Bethesda, MD) and cloned into pCDNA6 (Invitrogen, Carlsbad, CA), as described previously (*26*). The cDNA clone for $G\alpha_q$ was obtained from M. I. Simon (California Institute of Technology, Pasadena, CA).

Mutagenesis and Nomenclature. The residues histidine 335, leucine 336, phenylalanine 337, histidine 338, glutamate 339, leucine 340, valine 341, glutamine 342, arginine 343, and phenylalanine 344 within the C-terminal region of OTR were mutated to alanine using GeneEditor. Sequence changes were verified by DNA sequencing. To allow comparison of comparable residues between different receptors, in this study we adopted a consensus numbering scheme for GPCRs (*27*). In this system, the highly conserved proline within helix 7 of OTR is designated as 7.50; therefore, OTR residues H335, L336, F337, H338, E339, L340, V341, Q342, R343, and F344 are designated H7.59, L7.60, F7.61, H7.62, E7.63, L7.64, V7.65, Q7.66, R7.67, and F7.68, respectively.

Cell Culture and Transfection. COSM6 cells were cultured in Dulbecco's modified Eagle's medium (DMEM) containing 8% fetal calf serum (FCS), 2 mM L-glutamine, 50 units/mL penicillin, and 50 mg/mL streptomycin. For binding assays, COSM6 cells were plated at a density of 9×10^5 cells/100 mm dish. The next day, plasmid DNA (4.8 μg/dish) was mixed with 27 μL of Transfast in 5.4 mL of DMEM and incubated for 15 min before being added to the dish. After 1 h, 5.4 mL of DMEM containing 16% FCS was added to each dish, and the cells were harvested 48 h later. For phosphatidylinositide (PI) turnover experiments, COSM6 cells were plated into six-well plates (Corning Inc., Corning, NY) at a density of 1.5×10^5 cells/well. Receptor plasmid DNA (0.1−0.8 μg/well as indicated) and 0.01−0.08 μg of $G\alpha_q$ plasmid DNA were mixed with 4.5 μL of Transfast in 0.9 mL of DMEM and the cells treated as described above.

Membrane Preparation. Forty-eight hours after transfection, COSM6 cells were washed twice with phosphate-buffered saline (PBS) and harvested in chilled hypotonic buffer [20 mM HEPES (pH 7.4) and 10 mM EDTA]. The cells were homogenized at 4 °C for 3 × 10 s with a Polytron (Brinkmann). The homogenate was spun at 500*g* at 4 °C for 10 min, and the resulting supernatants were spun at 20000*g* and 4 °C for 30 min. The resulting crude membrane pellets were suspended in 20 mM HEPES buffer (pH 7.4) and stored in aliquots at −80 °C. The amount of protein was determined using the Bradford reagent (Bio-Rad) with BSA as the standard.

Ligand Binding Assay. Stored membranes were thawed, centrifuged (20000*g* for 30 min), and resuspended at a concentration of 0.1−0.2 mg of protein/mL in binding buffer [50 mM Tris (pH 7.4), 0.1% BSA, and 10 mM $MgCl_2$]. [^{3}H]-Oxytocin ([^{3}H]OT) was diluted in binding buffer. The binding assay mixtures (200 μL) containing cell membranes (10−20 μg of protein/well) and increasing concentrations of [^{3}H]OT (total binding) were incubated in Multiscreen filter plates with shaking for 2 h at room temperature. The level of nonspecific binding was determined by binding of [^{3}H]-OT and 10^{-5} M unlabeled OT ([^{3}H]OT at 0.03−10 nM) or by [^{3}H]OT binding in the membrane from cells transfected with the empty pCDNA6 vector ([^{3}H]OT at 10−600 nM). The plate was then mounted upon a Millipore vacuum manifold. The binding reaction was stopped by rapid filtration under vacuum to separate the bound ligand from the free, followed by two washes with cold binding buffer without $MgCl_2$. The filters containing the bound isotope were punched out and counted in Scintisafe Econo 1 (Fisher, Fairlawn, NJ). The level of specific binding was calculated as the difference between the total and nonspecific levels of binding.

PI Turnover. Twenty-four hours after transfection, COSM6 cells were washed twice with PBS, placed in 1 mL of DMEM containing 0.5% fetal calf serum and 0.4 μM [^{3}H]myoinositol, and incubated at 37 °C overnight. The labeled cells were washed twice with PBS and were incubated with Hank's Balanced Salt Solution (pH 7.4) containing 0.2% BSA and 10 mM LiCl at 37 °C for 30 min. The cells were stimulated for an additional 30 min with 10^{-10}−10^{-6} M oxytocin. [^{3}H]-Inositol 1,4,5-triphosphate (IP_3) was isolated by ion exchange chromatography (*28*). Data are expressed as OT-dependent activity.

Western Blot Analysis of Receptor Expression. Crude membranes from COSM6 cells transiently transfected with the pCDNA6 vector or the plasmids expressing OTR or the multiple-alanine substitution mutants were dissolved in electrophoresis sample buffer (*26*). Membrane proteins (10−20 μg) were separated on 10% SDS−PAGE gels and transferred onto nitrocellulose membranes. OTR antibodies (specific for the N- or C-terminus) were mixed and used at a 1:1000 dilution for each, and the PKA catalytic subunit (used to assess equal loading) was used at a 1:2000 dilution. Bands were detected by enhanced chemiluminescence (Amersham Biosci).

Immunocytochemistry and Confocal Microscopy. COSM6 cells were plated into two-well glass chambers (Nunc, Naperville, IL) at a density of 1.2×10^5 cells/well. The next day, 0.8 μg of the pCDNA6 vector or plasmids encoding OTR, OTR-(E7.63,R7.67)/A, or OTR-(H7.59,E7.63,R7.67)/A were applied for transfection with the protocol described above. Forty-eight hours after transfection, the cells were washed twice with cold PBS and were stained with Alexa 594-conjugated Con A (4 μg/mL) on ice for 30 min to localize the plasma membrane. After two brief washes with cold PBS, the cells were fixed with 4% paraformaldehyde in PBS for 10−15 min on ice. After two additional washes with PBS, the fixed cells were blocked with PBS containing 3% BSA for 1 h. Then the cells were incubated with the OTR antibody (specific for the N-terminus, 1:200 dilution in blocking buffer) at 4 °C overnight. After three washes with blocking buffer, the cells were labeled for 1 h with FITC-conjugated anti-goat antibody (1:300 dilution in blocking buffer). After two more washes with blocking buffer containing 0.025% Triton X-100, the slides with cell patches were mounted with coverslips.

Fluorescent images within the same optical field for both Con A (543 nm) staining and OTR (488 nm) immunostaining were acquired in an epifluorescence mode under a 60× magnifying oil lens of an LSM 510 confocal laser scanning microscope (Zeiss). The acquired images were exported to Adobe PhotoShop for further processing.

Data Analysis. Binding data were analyzed with the Ligand program (P. J. Munson, National Institute of Child Health and Human Development, National Institutes of Health, Bethesda, MD). Dose−response curves of PI turnover were analyzed with a four-parameter logistics curve fitting program (M. L. Jaffe, Silver Spring, MD). Data are presented as the mean ± the standard error and were analyzed by ANOVA and Duncan's modified multiple range tests or unpaired *t* tests where appropriate.

RESULTS

A Putative α-Helical Structure (Helix 8) Is Predicted within the Membrane-Proximal Region of the OTR C-Terminal Domain. The crystal structure of bovine rhodopsin in the dark state revealed an 11-amino acid α-helical structure (helix 8) near the extension of transmembrane helix 7 (*18*). Using several secondary structure prediction programs, we found putative α-helical structures within the C-terminal domains of both OTR and V_2R. When the highly conserved NPxxY motif and double cysteine pair of OTR, V_2R, and bovine rhodopsin were aligned, putative helix 8 structures for both OTR and V_2R, designated in bold in Figure 1A, were located in the same area as the residues of rhodopsin helix 8. Helical wheel projections of the residues in putative helix 8 of both OTR and V_2R revealed an amphipathic arrangement, with hydrophilic residues on one side and hydrophobic residues on another side. Five hydrophilic residues, including H7.59, H7.62, E7.63, Q7.66, and R7.67, comprised the hydrophilic face of the putative helix 8 of OTR. The size of the hydrophilic face of the corresponding V_2R helix was larger than that for OTR. We postulated that the hydrophobic face of OTR might interact with the plasma membrane, while the hydrophilic face might face the cytoplasm to interact with G-proteins.

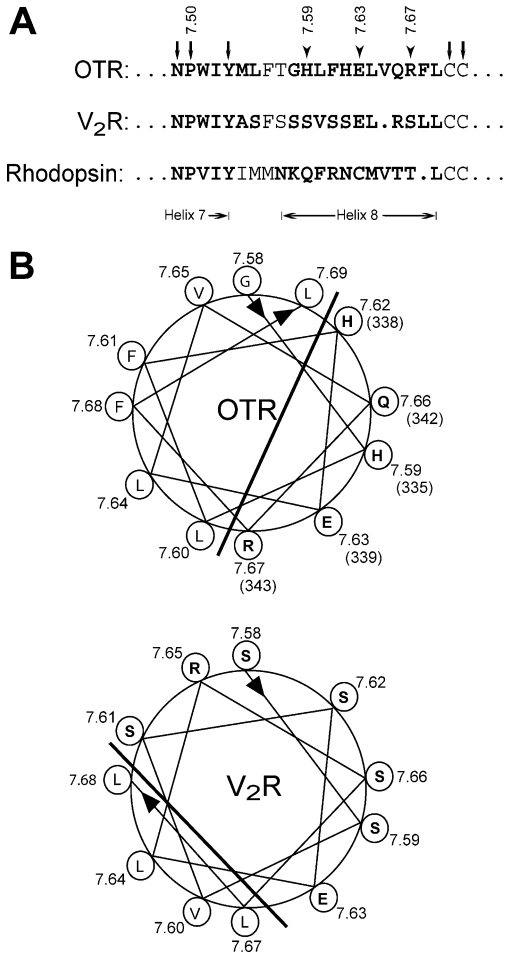

FIGURE 1: (A) Secondary structure and sequence alignment of human OTR, rat V_2R, and bovine rhodopsin. The residues within the predicted helices of OTR and V_2R (psi-pred prediction program) and helix 8 of bovine rhodopsin (PDB entry 1F88) are designated with bold letters. Residues designated with arrows are conserved within the class A GPCR family, while those designated with arrowheads are important to the function of OTR. The proline of the conserved NPxxY motif in helix 7 is designated as residue 7.50 (*27*). (B) Helical wheel projections of the putative helix 8 structures of OTR and V_2R. The solid line separates the hydrophilic and hydrophobic sides of the amphipathic helices. Hydrophilic amino acids are designated with bold letters.

Residues H7.59, E7.63, and R7.67 Are Important for Preserving both Receptor Affinity for Oxytocin and Signal Transduction. To explore the potential influence of residues in the hydrophilic face of putative helix 8 on OTR function, residues were individually changed into alanine and the functional properties of the resulting mutant receptors assessed. Equal amounts of plasmid DNA for wild-type OTR and five alanine substitution mutants (H7.59/A, H7.62/A, E7.63/A, Q7.66/A, and R7.67/A) were expressed in COSM6 cells. Representative binding curves are shown in Figure 2A; binding parameters are summarized in Table 1. Wild-type OTR in COSM6 membranes exhibited high-affinity binding of [^{3}H]OT (K_d = 0.52 nM). Alanine substitution at position H7.62 (OTR-H7.62/A) or Q7.66 (OTR-Q7.66/A) resulted in OTR mutants with affinity comparable to that of wild-type OTR (K_d = 0.48−0.63 nM), whereas the affinities of OTR-H7.59/A, OTR-E7.63/A, and OTR-R7.67/A were lower (K_d = 2.61−3.15 nM) than that of wild-type OTR. The expression levels of each of these mutant receptors were similar but were roughly 50% of that of wild-type OTR.

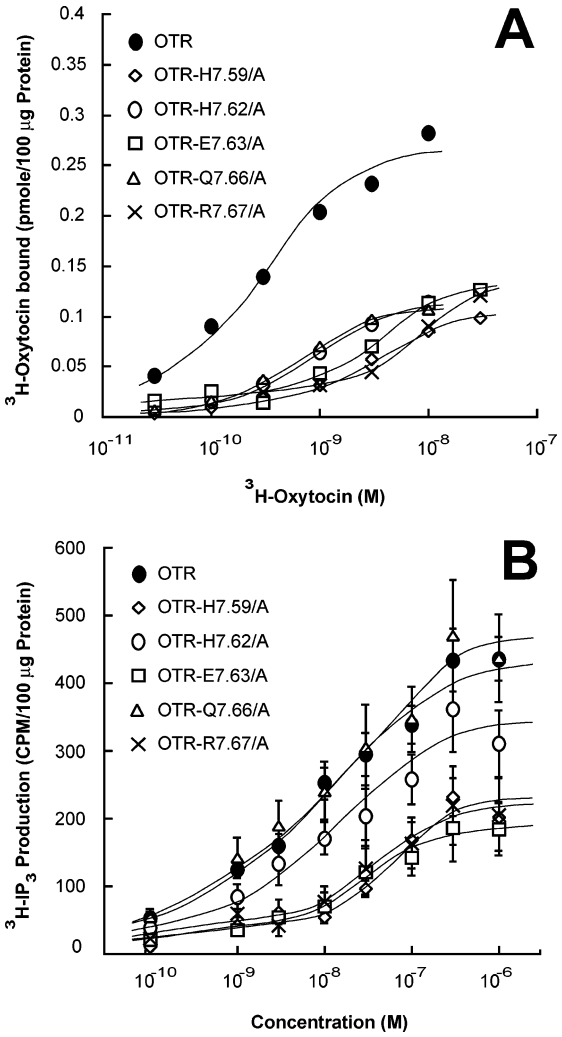

FIGURE 2: Single alanine substitution for the residues within the hydrophilic interface of putative helix 8 of OTR decreases the receptor's affinity for OT and attenuates its response to activate PLC. Panel A shows representative binding curves of wild-type OTR and alanine substitution mutants in one of four similar experiments. Panel B shows the capacities of these receptors, expressed at equal concentrations as described in Table 1, to activate PLC in response to OT stimulation. Data are expressed as the mean ± the standard error of six experiments.

Under transfection conditions where equal amounts of OTR and mutant receptors were expressed, OT-stimulated [^{3}H]IP$_3$ formation by wild-type OTR and mutant receptors was evaluated. The data are summarized in Table 1, and representative dose−response curves are plotted in Figure 2B. There were no significant differences in the EC_{50} values between wild-type OTR and the five mutant receptors. The maximum responses of OTR-H7.62/A and OTR-Q7.66/A to OT were similar to that of wild-type OTR. In contrast, alanine substitution for H7.59, E7.63, or R7.67 resulted in mutant receptors with weakened ability to activate PLC; maximum responses to OT stimulation were ~50% of that of wild-type OTR. Therefore, residues H7.59, E7.63, and R7.67, but not H7.62 or Q7.66, have important influences on OTR function.

Multiple Alanine Substitutions for H7.59, E7.63, or R7.67 Result in the Loss of Function of OTR. To determine whether the replacement of alanine at more than one of the implicated residues further altered OTR function, we constructed double and triple alanine substitutions to produce mutant receptors OTR-(H7.59,E7.63,R7.67)/A, OTR-(H7.62,Q7.66)/A, OTR-(H7.59,E7.63)/A, OTR-(H7.59,R7.67)/A, and OTR-(E7.63,R7.67)/A. Representative binding data for these receptors are shown in panels A and B of Figure 3, and binding parameters are summarized in Table 2. Alanine substitutions for H7.62 and Q7.66 produced a receptor with a high affinity for [^{3}H]OT (0.75 nM) but reduced the level of receptor membrane expression to approximately 30% of that of wild-type OTR. These data indicated that the binding site for OT was relatively intact in the OTR-(H7.62,Q7.66)/A mutant. In sharp contrast, Figure 3A shows that alanine modifications for two or more of the residues (H7.59, E7.63, and R7.67) completely eliminated the high-affinity membrane binding site for OT, while retaining low-affinity binding (Figure 3B), suggesting that the receptors were probably still present but altered in configuration. This low-affinity binding was receptor transfection-dependent relative to the empty vector. Low-affinity binding of [^{3}H]OT to wild-type OTR was also observed (Figure 3B), and was not saturable at the concentrations that were used.

Figure 4A shows that, in addition to wild-type OTR, the mutant receptors were expressed in the crude membrane fraction from transiently transfected COSM6 cells. Cells transiently transfected with the pCDNA6 vector did not exhibit a specific OTR band, while a 70 kDa band was detected with anti-OTR antibodies in samples from cells expressing wild-type and mutant receptors. The PKA catalytic subunit was used as an internal protein loading control. To determine further whether these alanine modifications affected the trafficking of OTR to the plasma membrane, we immunostained COSM6 cells transiently expressing OTR-(E7.63,R7.67)/A or OTR-(H7.59,E7.63,R7.67)/A, together with cells transiently transfected with the pCDNA6 vector or OTR-expressing plasmid as negative and positive controls. Cells were prestained with Alexa 594-conjugated Con A to visualize the plasma membrane before being fixed

Table 1: Pharmacological Profile of Wild-Type OTR and Single-Alanine Substitution Mutants in the Hydrophilic Interface of Putative Helix 8 of OTR[a]

	[^{3}H]OT binding		OT-stimulated IP$_3$ formation	
receptor	K_d (nM)	B_{max} (fmol/100 μg of protein)	EC_{50} (nM)	R_{max} (cpm/100 μg of protein)
OTR	0.52 ± 0.09[a]	287 ± 70[a]	18.3 ± 3.4[a]	503 ± 35[a]
OTR-H7.59/A	3.15 ± 1.27[b]	95 ± 9[b]	33.8 ± 9.4[a]	232 ± 33[b]
OTR-H7.62/A	0.63 ± 0.07[a]	91 ± 10[b]	20.6 ± 7.6[a]	347 ± 63[a,b]
OTR-E7.63/A	2.61 ± 1.39[b]	129 ± 25[b]	31.2 ± 8.9[a]	206 ± 44[b]
OTR-Q7.66/A	0.48 ± 0.05[a]	100 ± 17[b]	15.9 ± 5.7[a]	496 ± 79[a]
OTR-R7.67/A	3.04 ± 0.96[b]	144 ± 33[b]	38.9 ± 14.8[a]	231 ± 60[b]

[a] The receptor plasmids were transiently transfected into COSM6 cells. For membrane binding assays, an equal amount of plasmid DNA (4.8 μg/100 mm dish) was transfected for each receptor. The maximal binding (B_{max}) and receptor affinity (K_d) were calculated with the Ligand program and are reported as the mean ± the standard error ($n = 4$). For phosphatidylinositide turnover, the concentration of expressed receptors was normalized (the B_{max} for OTR is 139 ± 51 fmol of binding sites/100 μg of protein, $n = 4$) by adjusting the amount of transfected plasmid DNA (0.45 μg/well for OTR and 0.8 μg/well for the mutant receptors). Maximal ligand-stimulated response (R_{max}) and EC_{50} values were calculated with a four-parameter logistics curve fitting program and are reported as the mean ± the standard error ($n = 6$). K_d and EC_{50}, but not B_{max} or R_{max}, were log-transformed for analysis; all parameters were analyzed by ANOVA and Duncan's modified range test. Significant differences between groups in a given category ($P < 0.05$) are designated with different lowercase letters.

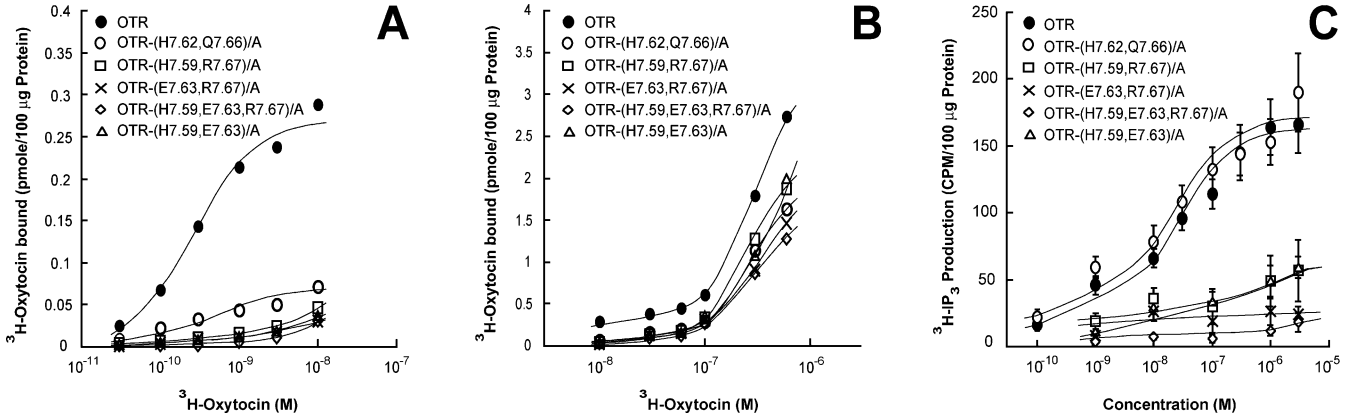

FIGURE 3: Multiple alanine substitutions for the residues within the hydrophilic interface of putative helix 8 of OTR eliminate both high-affinity OT binding and the ability to activate PLC. Panel A shows representative binding curves of wild-type OTR and alanine substitution mutants in one of four similar experiments. Panel B shows the low-affinity binding of wild-type and mutant oxytocin receptors. Panel C shows the capacities of these receptors to activate PLC in response to OT stimulation under the conditions described in Table 2. Data are expressed as the mean ± the standard error of six experiments.

Table 2: Pharmacological Profile of Wild-Type OTR and Multiple-Alanine Substitution Mutants in the Hydrophilic Interface of Putative Helix 8 of OTR[a]

	[^{3}H]OT binding		OT-stimulated IP$_3$ formation	
receptor	K_d (nM)	B_{max} (fmol/100 μg of protein)	EC_{50} (nM)	R_{max} (cpm/100 μg of protein)
OTR	0.52 ± 0.09	287 ± 70	38.5 ± 8.5	186 ± 25
OTR-(H7.62,Q7.66)/A	0.75 ± 0.06	86 ± 21[b]	44.5 ± 13.7	209 ± 30
OTR-(H7.59,E7.63)/A	nd	nd	nd	nd
OTR-(H7.59,R7.67)/A	nd	nd	nd	nd
OTR-(E7.63,R7.67)/A	nd	nd	nd	nd
OTR-(H7.59,E7.63,R7.67)/A	nd	nd	nd	nd

[a] For membrane binding assays, an equal amount of plasmid DNA (4.8 μg/100 mm dish) was transfected for each receptor. The maximal binding (B_{max}) and receptor affinity (K_d) were calculated with the Ligand program and are reported as the mean ± the standard error ($n = 4$). For the phosphatidylinositide turnover assay, the expression levels of OTR and OTR-(H7.62,Q7.66)/A were normalized (the B_{max} for OTR is 95 ± 24 fmol of binding sites/100 μg of protein, $n = 4$) by adjusting the amount of transfected plasmid DNA (0.1 μg/well for OTR and 0.8 μg/well for the mutant receptor). A similar concentration of DNA was used for the other receptors; this resulted in the expression of the same amount of low-affinity binding for all mutant receptors between 50 and 500 nM [^{3}H]OT. Maximal ligand-stimulated response (R_{max}) and EC_{50} values were calculated with a four-parameter logistics curve fitting program and are reported as the mean ± the standard error ($n = 6$). The data were analyzed with an unpaired *t* test. Values that did not show saturation (binding) or elicit sufficient OT dose dependence (PI turnover) to be analyzed are designated as not determinable (nd). [b] $P < 0.01$.

with 4% paraformaldehyde. Immunostaining for OTR was performed under cell-impermeable conditions. The results shown in Figure 4B are consistent with the observations obtained by Western blotting. Cells transiently transfected with the empty pCDNA6 vector were negative for anti-OTR antibody staining, whereas the specific fluorescence that indicates the presence of OTR was shown on the plasma membrane of cells expressing wild-type OTR as well as OTR-(E7.63,R7.67)/A or OTR-(H7.59,E7.63,R7.67)/A. The fluorescence of wild-type and mutant OTRs colocalized with Con A fluorescence, consistent with expression of the OTR constructs on the cell plasma membrane. These data provide additional support for the idea that the alanine modifications in the C-terminal domain of OTR, while altering expression and function, did not prevent localization of the receptor on the cell surface.

We adjusted the amount of transfected OTR plasmid DNA so that it was expressed at a concentration equal to that of OTR-(H7.62,Q7.66)/A and used the same conditions for the other double and triple mutants. The parameters associated with OT-stimulated IP_3 formation are summarized in Table 2, and representative dose−response curves are plotted in Figure 3C. Consistent with its high affinity for OT, OTR-(H7.62,Q7.66)/A responded to OT stimulation as well as wild-type OTR with respect to both EC_{50} and maximum response. All of the double mutants involving alanine modification at positions H7.59, E7.63, and R7.67 and the triple mutant exhibited little or no ability to activate PLC. Any residual activity was OT- but not dose-dependent (ANOVA analysis, $P > 0.05$). The data again point to an important function of the putative helix 8 face containing H7.59, E7.63, and R7.67 for OTR function.

Residues in the Hydrophobic Face of Putative Helix 8 Are Not Essential for the Function of OTR. The hydrophobic face of putative helix 8 of OTR is composed of seven amino acid residues, with glycine 7.58 at the loop−helix transition junction and L7.69 at the end of putative helix 8. In this study, we created three alanine substitution mutants [OTR-(L7.60,F7.61)/A, OTR-(L7.64,V7.65)/A, and OTR-F7.68/A] that covered five residues in the hydrophobic face of putative helix 8 of OTR. Representative binding curves are shown in Figure 5A, and binding parameters are summarized in Table 3. Alanine modifications in this hydrophobic face reduced the level of membrane expression of mutant receptors to a comparable degree, approximately 50% of that of wild-type OTR. None of the alanine substitutions in this hydrophobic face affected high-affinity binding for [^{3}H]OT (K_d = 1.69−2.64 nM), compared with that for wild-type OTR (K_d = 1.09 nM).

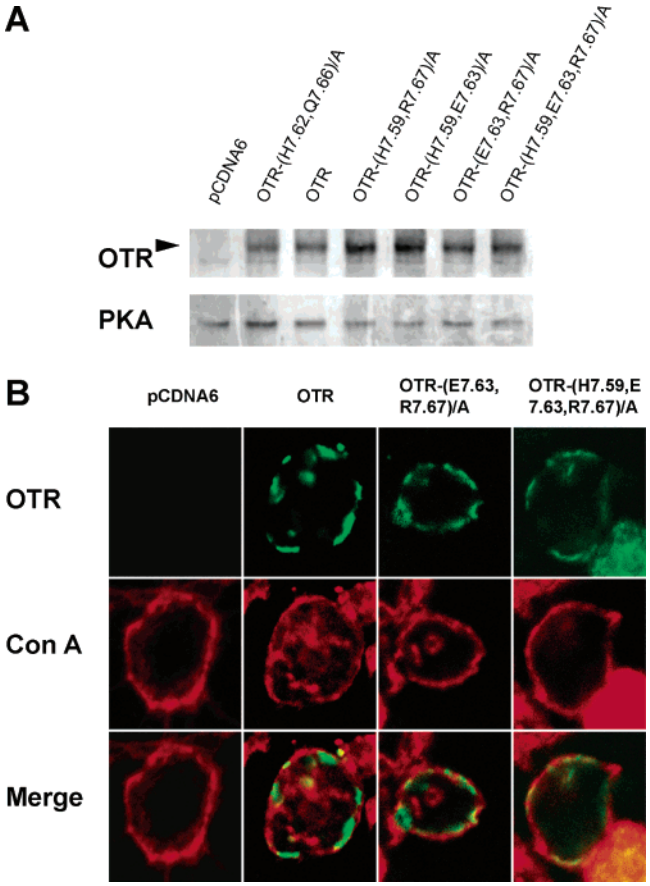

FIGURE 4: Expression and localization of wild-type OTR and the multiple-alanine substitution mutant receptors in transfected COSM6 cells. Panel A shows that proteins present in crude membrane preparations from transfected COSM6 cells were detected with anti-OTR antibodies. The PKA catalytic subunit was used as an internal loading control on the same blot following stripping. Panel B shows the expression and cellular localization of wild-type OTR and the OTR-(E7.63,R7.67)/A and OTR-(H7.59,E7.63,R7.67)/A mutant receptors by immunostaining of the nonpermeabilized fixed cells with the anti-OTR antibody (specific for the N-terminus) together with the FITC-conjugated secondary antibody. The plasma membrane was localized by prestaining with Alexa 594-conjugated Con A before cell fixation. Cells transiently transfected with the pCDNA6 vector was used as a negative control.

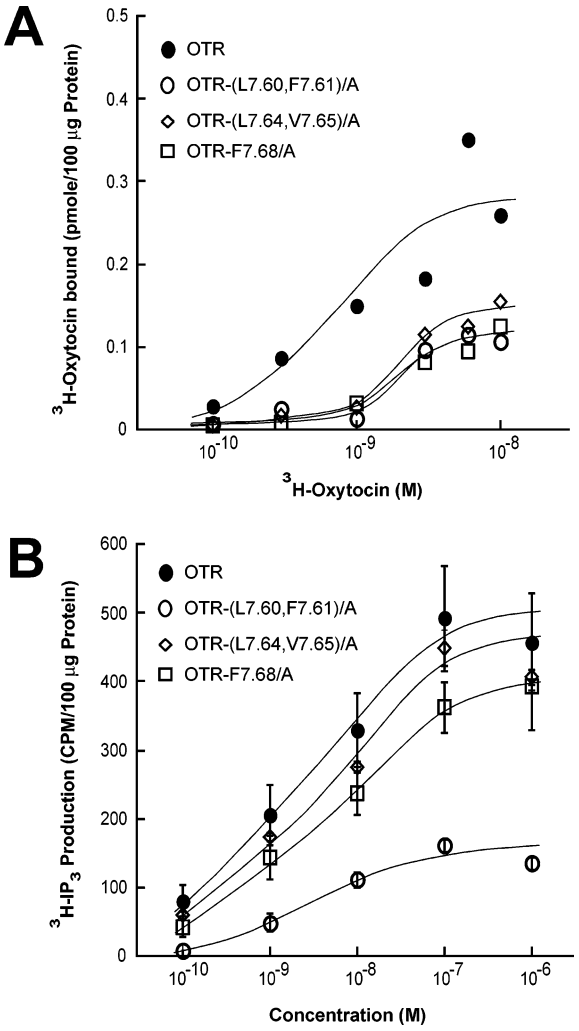

FIGURE 5: Residues in the hydrophobic interface of putative helix 8 are not essential for preserving both the OTR conformation and its ability to activate PLC. Panel A shows representative binding curves of wild-type OTR and alanine substitution mutants in one of three similar experiments. Panel B shows the capacities of these receptors, expressed at equal concentrations as described in Table 3, to activate PLC in response to OT stimulation. Data are expressed as the mean ± the standard error of three experiments.

The expression of wild-type OTR was normalized to the level of the mutant receptors by adjusting the amounts of transfected plasmid DNA. The parameters associated with OT-stimulated IP_3 formation are summarized in Table 3, and representative dose−response curves are plotted in Figure 5B. Alanine modifications at L7.64 and V7.65 or at F7.68 did not significantly affect the response of the mutant receptors to OT stimulation, as was reflected in both the EC_{50} and maximum response. Alanine substitutions for L7.60 and F7.61 resulted in a mutant receptor that responded to OT stimulation with an EC_{50} comparable to that of wild-type OTR, but an impaired maximum response (~30% of that of wild-type OTR).

DISCUSSION

GPCRs share a seven-transmembrane α-helical structure, with the amino terminus on the extracellular side and the carboxyl terminus on the intracellular side of the plasma membrane. Despite the structural variety of their ligands, some members of the class A GPCR family have been shown to undergo a conserved activation mechanism (*29*, *30*). However, this observation is not likely to extend to the role of the C-terminal domain, because the phenotypes of different class A GPCRs with C-terminal modifications are varied. In human β_2-adrenergic receptor, the N-terminal segment of the cytoplasmic tail was critical for productive coupling of the receptor to G-proteins (*15*), whereas a truncated rat neurokinin-1 receptor lacking the carboxyl-terminal region was indistinguishable from its wild-type receptor with respect to substance P-induced accumulation of [^{3}H]IP_3 (*31*). At least four isoforms of the prostaglandin EP3 receptor, produced by alternative splicing with differences only in their carboxyl-terminal domains, coupled to different G-proteins to activate different second messenger systems (*32*). Mammalian GnRH receptor coupled effectively to $G\alpha_{q/11}$ despite lacking a C-terminal domain (*16*, *17*); a rat GnRH receptor chimera possessing the C-terminal tail of bullfrog GnRH receptor had impaired capacity to couple to $G\alpha_{q/11}$ (*33*). It appears that the influence of the C-terminal domain of class A GPCRs on their function depends on the local microenvironment that is unique to the particular receptor that is studied.

Table 3: Pharmacological Profile of Wild-Type OTR and Alanine Substitution Mutants in the Hydrophobic Interface of Putative Helix 8 of OTR[a]

	[^{3}H]OT binding		OT-stimulated IP_3 formation	
receptor	K_d (nM)	B_{max} (fmol/100 μg of protein)	EC_{50} (nM)	R_{max} (cpm/100 μg of protein)
OTR	1.09 ± 0.53^a	298 ± 31^a	3.3 ± 0.8^a	489 ± 78^a
OTR-(L7.60,F7.61)/A	2.64 ± 0.48^a	136 ± 8^b	2.9 ± 1.0^a	148 ± 5^b
OTR-(L7.64,V7.65)/A	2.09 ± 0.56^a	144 ± 17^b	4.1 ± 1.3^a	442 ± 17^a
OTR-F7.68/A	1.69 ± 0.50^a	138 ± 27^b	5.7 ± 1.4^a	435 ± 88^a

[a] For membrane binding assays, an equal amount of plasmid DNA (4.8 μg/100 mm dish) was transfected for each receptor. The maximal binding (B_{max}) and receptor affinity (K_d) were calculated with the Ligand program and are reported as the mean $\pm$ the standard error ($n = 3$). For the phosphatidylinositide turnover assay, the expression level of OTR was normalized to the level of the mutant receptors (the B_{max} for OTR is 167 fmol of binding sites/100 μg of protein, $n = 1$) by adjusting the amount of transfected plasmid DNA (0.4 μg/well for OTR and 0.8 μg/well for the mutant receptors). Maximal ligand-stimulated response (R_{max}) and EC_{50} values were calculated with a four-parameter logistics curve fitting program and are reported as the mean $\pm$ the standard error ($n = 3$). A different preparation of the plasmid encoding $G\alpha_q$ was used for the experiments described in Table 3 and those in Tables 1 and 2; this may explain the differences in the EC_{50} value for OTR. The data were analyzed by ANOVA and Duncan's modified range test. Significant differences between groups in a given category ($P < 0.05$) are designated with different lowercase letters.

In OTR, Hoare et al. identified a segment (E7.63−R7.74) within its C-terminal domain that is important for selective activation of $G\alpha_q$ (*25*). In contrast, we found that a 36-amino acid sequence from the C-terminal region of the third cytoplasmic domain of OTR could convey an enhanced ability to stimulate PLC to a V_2R−OTR chimera (*28*). Furthermore, mutation of a single residue, K6.30, in this segment to valine eliminated the ability of both native OTR and this V_2R chimera to activate PLC but had no effect on the ability of the V_2R chimera to stimulate adenylate cyclase. These data point to the particular importance of this third intracellular domain residue in OTR−$G\alpha_q$ coupling. Since there is little homology between V_2R and OTR in their C-terminal domains, either sequence in this region does not play an essential role in $G\alpha_q$ coupling in these receptors, or the contribution of the C-terminal domain to G-protein coupling in the V_2R chimera can be provided by the wild-type V_2R sequence.

The crystal structure of bovine rhodopsin revealed the presence of helix 8 (*18*). The amino terminus of helix 8 of rhodopsin has been implicated in the activation of $G\alpha_t$ as a result of interaction with residues in its carboxyl terminus (*34*, *35*). Site-directed spin-labeling studies provided evidence of a light- and activation-dependent transition of this helix into a looplike structure (*36*). Furthermore, a peptide corresponding to the helix 8 region of rhodopsin adopted a looplike structure in solution (*37*). Biophysical studies showed that the rhodopsin helix 8 peptide bound to liposomes of almost any phospholipid composition, but it formed a helix only in the presence of acidic phosphatidylserine lipids (*38*). These studies suggest that the fourth cytoplasmic segment of rhodopsin exists in distinct conformations that are sensitive to both light activation and changes in membrane lipid composition. Similarly, ^{1}H NMR spectroscopy showed that a peptide consisting of the C-terminal membrane-proximal region of β-adrenergic receptor (P7.57−F7.69) adopted an amphipathic α-helix only in the presence of lysomyristoylphosphatidylcholine micelles (*19*). An amphipathic α-helical solution structure was also observed in the C-terminal fragment (L7.56−T7.70) of rat angiotensin II type 1A receptor; the extension of the α-helix within this region was dependent on the polarity of the medium (*20*). Since the α-helical regions within the C-terminal tails of these GPCRs, bounded on one side by helix 7 and on the other by two fatty acylated cysteine residues, are expected to be at the membrane interface, the membrane composition may have an important influence on the conformation of this segment of the receptor sequence. It is interesting in this regard that OTR properties are altered when the receptor is placed in environments with different lipid compositions (*39*, *40*).

In the study presented here, we identified by computer analysis a putative amphipathic α-helical structure (helix 8) in the membrane-proximal region of the OTR cytoplasmic tail (G7.58−L7.69). Interestingly, the comparable segment of V_2R also forms a putative amphipathic helix, suggesting that features of this structure, rather than a linear sequence, may be what is required to enhance G-protein coupling. Residues in the hydrophilic face of the predicted helix 8 of OTR were shown to be critical for preserving the receptor conformation, as reflected in agonist binding affinity and activation of PLC. Three hydrophilic amino acid residues (H7.59, E7.63, and R7.67) played a dominant role, while H7.62 and Q7.66 served as negative controls. Single alanine replacement of H7.59, E7.63, or R7.67 significantly reduced the affinity of OTR for OT. Changing H7.62 and Q7.66 to alanine preserved the high affinity for ligand without affecting PLC activation, whereas mutation of E7.63 and R7.67, the neighbors of H7.62 and Q7.66, respectively, in the linear sequence, eliminated the high-affinity binding site for OT while preserving the low-affinity binding that has been observed previously (*41*). In fact, mutation of any two or more of the residues (H7.59, E7.63, and R7.67) produced receptors that lost high-affinity binding; none were able to respond to OT with a dose-dependent activation of PLC. These data are consistent with the importance of a specific region in the hydrophilic face of the putative helix 8 in OTR function.

Helix 8 of bovine rhodopsin is oriented at 90° with respect to the other transmembrane helices in the crystal structure and is close to the residues of the cytoplasmic ends of helices 1, 2, and 6 (*18*). Disulfide bond formation between engineered cysteine pairs showed that H65(1.60)/C at the cytoplasmic end of helix 1 had a 6-fold greater potential to interact with C316(7.63) in helix 8 than with any other residues located there (*36*). The comparable residue in OTR is E339(7.63), which we have implicated in OTR function. On the basis of significant conservation of residues in the seven transmembrane helices and C-terminal domain of class A GPCRs, it has been suggested that the orientation of transmembrane helical bundles and packing of these receptors

are relatively conserved (*42*). Accordingly, although the level of overall homology between OTR and rhodopsin sequences is less than 25%, we postulate that the hydrophilic face of putative helix 8 of OTR that includes H7.59, E7.63, and R7.67 may interact with residues on the cytoplasmic end of helix 1. This could affect the orientation of helix 1 relative to the other helices. Hence, mutation of these residues could indirectly affect both ligand binding and the ability to interact with or activate G-proteins. Alternatively, substitution of alanine for the hydrophilic residues also reduced the size of the putative hydrophilic interface. Therefore, these modifications might interrupt this putative helix 8−lipid interaction pattern and alter OTR function. Finally, some residues may also interact with the C-terminal region of G-protein α-subunits.

In the crystal structure of bovine rhodopsin, some of the residues in the hydrophobic face of helix 8 are adjacent to helix 7 due to the unique helix−turn−helix folding in this region. Among them, F7.60 in helix 8 has been shown to form a local constraint in rhodopsin by hydrophobic interaction with Y7.53 in the conserved NPxxY motif of helix 7 (*10*). Alanine substitution for either Y7.53 or F7.60 to disrupt this constraint results in formation of the meta II active state; a disulfide bond cross-linking of residues at positions 7.53 and 7.60 prevents receptor isomerization into the meta II state (*10*). In serotonin type 2C receptor, an interhelical module involving Y7.53 and Y7.60 has also been found to influence the switching among multiple active and inactive conformations (*11*). To investigate the potential influence of the hydrophobic face of this putative helix 8 on OTR function, we mutated five of its constituent residues to alanine (L7.60, F7.61, L7.64, V7.65, and F7.68). Alanine modification at positions L7.64 and V7.65 or F7.68 did not affect either the conformation of OTR or its function for signaling, as reflected in the K_d for [^{3}H]OT binding and capacities for IP_3 formation following activation by OT. These data exclude this hydrophobic portion of putative helix 8, including L7.64, V7.65, and F7.68, from OTR function. Alanine modification at L7.60 and F7.61 resulted in a mutant receptor that retained high-affinity binding for [^{3}H]OT but exhibited a weakened ability to activate PLC. This phenotype for the OTR-(L7.60, F7.61)/A mutant receptor is similar to that observed for the F7.60/A mutation in rhodopsin (*10*). This may indicate that, by analogy, either L7.60 or F7.61 in putative helix 8 of OTR may interact with hydrophobic residues in helix 7.

In summary, results of alanine scanning are consistent with the presence of a putative helix 8 within the membrane-proximal region of the C-terminus of OTR. The data suggest that three amino acids in the hydrophilic face are important to the role of this putative helix 8 in preserving the receptor conformation that is necessary for ligand binding and stimulation of G-protein-mediated PLC activation. Most alanine mutations in the hydrophobic face did not affect OT binding or impair the ability to activate PLC. Mutation of L7.60 and F7.61 to alanine weakened but did not eliminate the ability to stimulate PLC, in contrast to mutations on the hydrophilic face. Therefore, alanine substitutions in the hydrophilic interface may affect interhelical interactions within OTR or interactions with G-proteins by changing the microenvironment of putative helix 8.

ACKNOWLEDGMENT

We thank Mr. Mark Kao for his assistance in preparing the manuscript and Dr. Chun-Yin Ku for her advice on immunoblotting.

REFERENCES

1. Kimura, T., Tanizawa, O., Mori, K., Brownstein, M. J., and Okayama, H. (1992) Structure and expression of a human oxytocin receptor, *Nature 356*, 526−529.
2. Wess, J. (1998) Molecular basis of receptor/G-protein-coupling selectivity, *Pharmacol. Ther. 80*, 231−264.
3. Farrens, D. L., Altenbach, C., Yang, K., Hubbell, W. L., and Khorana, H. G. (1996) Requirement of rigid-body motion of transmembrane helices for light activation of rhodopsin, *Science 274*, 768−770.
4. Sheikh, S. P., Zvyaga, T. A., Lichtarge, O., Sakmar, T. P., and Bourne, H. R. (1996) Rhodopsin activation blocked by metal-ion-binding sites linking transmembrane helices C and F, *Nature 383*, 347−350.
5. Gether, U., Lin, S., Ghanouni, P., Ballesteros, J. A., Weinstein, H., and Kobilka, B. K. (1997) Agonists induce conformational changes in transmembrane domains III and VI of the β_2 adrenoceptor, *EMBO J. 16*, 6737−6747.
6. Javitch, J. A., Fu, D., Liapakis, G., and Chen, J. (1997) Constitutive activation of the β_2 adrenergic receptor alters the orientation of its sixth membrane-spanning segment, *J. Biol. Chem. 272*, 18546−18549.
7. Ghanouni, P., Steenhuis, J. J., Farrens, D. L., and Kobilka, B. K. (2001) Agonist-induced conformational changes in the G-protein-coupling domain of the β_2 adrenergic receptor, *Proc. Natl. Acad. Sci. U.S.A. 98*, 5997−6002.
8. Ward, S. D., Hamdan, F. F., Bloodworth, L. M., and Wess, J. (2002) Conformational changes that occur during M_3 muscarinic acetylcholine receptor activation probed by the use of an in situ disulfide cross-linking strategy, *J. Biol. Chem. 277*, 2247−2257.
9. Parnot, C., Bardin, S., Miserey-Lenkei, S., Guedin, D., Corvol, P., and Clauser, E. (2000) Systematic identification of mutations that constitutively activate the angiotensin II type 1A receptor by screening a randomly mutated cDNA library with an original pharmacological bioassay, *Proc. Natl. Acad. Sci. U.S.A. 97*, 7615−7620.
10. Fritze, O., Filipek, S., Kuksa, V., Palczewski, K., Hofmann, K. P., and Ernst, O. P. (2003) Role of the conserved NPxxY$(x)_{5,6}$F motif in the rhodopsin ground state and during activation, *Proc. Natl. Acad. Sci. U.S.A. 100*, 2290−2295.
11. Prioleau, C., Visiers, I., Ebersole, B. J., Weinstein, H., and Sealfon, S. C. (2002) Conserved helix 7 tyrosine acts as a multistate conformational switch in the $5HT_{2C}$ receptor. Identification of a novel "locked-on" phenotype and double revertant mutations, *J. Biol. Chem. 277*, 36577−36584.
12. Abdulaev, N. G., and Ridge, K. D. (1998) Light-induced exposure of the cytoplasmic end of transmembrane helix seven in rhodopsin, *Proc. Natl. Acad. Sci. U.S.A. 95*, 12854−12859.
13. Miura, S., Zhang, J., Boros, J., and Karnik, S. S. (2003) TM2-TM7 interaction in coupling movement of transmembrane helices to activation of the angiotensin II type-1 receptor, *J. Biol. Chem. 278*, 3720−3725.
14. Ferguson, S. S. (2001) Evolving concepts in G protein-coupled receptor endocytosis: the role in receptor desensitization and signaling, *Pharmacol. Rev. 53*, 1−24.
15. O'Dowd, B. F., Hnatowich, M., Regan, J. W., Leader, W. M., Caron, M. G., and Lefkowitz, R. J. (1988) Site-directed mutagenesis of the cytoplasmic domains of the human β_2-adrenergic receptor. Localization of regions involved in G protein-receptor coupling, *J. Biol. Chem. 263*, 15985−15992.
16. Eidne, K. A., Sellar, R. E., Couper, G., Anderson, L., and Taylor, P. L. (1992) Molecular cloning and characterisation of the rat pituitary gonadotropin-releasing hormone (GnRH) receptor, *Mol. Cell. Endocrinol. 90*, R5−R9.
17. Hsieh, K. P., and Martin, T. F. (1992) Thyrotropin-releasing hormone and gonadotropin-releasing hormone receptors activate phospholipase C by coupling to the guanosine triphosphate-binding proteins G_q and G_{11}, *Mol. Endocrinol. 6*, 1673−1681.
18. Palczewski, K., Kumasaka, T., Hori, T., Behnke, C. A., Motoshima, H., Fox, B. A., Le Trong, I., Teller, D. C., Okada, T., Stenkamp, R. E., Yamamoto, M., and Miyano, M. (2000) Crystal

structure of rhodopsin: A G protein-coupled receptor, *Science 289*, 739−745.
19. Jung, H., Windhaber, R., Palm, D., and Schnackerz, K. D. (1996) Conformation of a β-adrenoceptor-derived signal transducing peptide as inferred by circular dichroism and ^{1}H NMR spectroscopy, *Biochemistry 35*, 6399−6405.
20. Franzoni, L., Nicastro, G., Pertinhez, T. A., Tato, M., Nakaie, C. R., Paiva, A. C., Schreier, S., and Spisni, A. (1997) Structure of the C-terminal fragment 300−320 of the rat angiotensin II AT_{1A} receptor and its relevance with respect to G-protein coupling, *J. Biol. Chem. 272*, 9734−9741.
21. Arnaudeau, S., Lepretre, N., and Mironneau, J. (1994) Oxytocin mobilizes calcium from a unique heparin-sensitive and thapsigargin-sensitive store in single myometrial cells from pregnant rats, *Pfluegers Arch. 428*, 51−59.
22. Ku, C. Y., Qian, A., Wen, Y., Anwer, K., and Sanborn, B. M. (1995) Oxytocin stimulates myometrial guanosine triphosphatase and phospholipase-C activities via coupling to $G\alpha_{q/11}$, *Endocrinology 136*, 1509−1515.
23. Strakova, Z., and Soloff, M. S. (1997) Coupling of oxytocin receptor to G proteins in rat myometrium during labor: G_i receptor interaction, *Am. J. Physiol. 272*, E870−E876.
24. Baek, K. J., Kwon, N. S., Lee, H. S., Kim, M. S., Muralidhar, P., and Im, M. J. (1996) Oxytocin receptor couples to the 80 kDa G_h α family protein in human myometrium, *Biochem. J. 315* (Part 3), 739−744.
25. Hoare, S., Copland, J. A., Strakova, Z., Ives, K., Jeng, Y. J., Hellmich, M. R., and Soloff, M. S. (1999) The proximal portion of the COOH terminus of the oxytocin receptor is required for coupling to G_q, but not G_i. Independent mechanisms for elevating intracellular calcium concentrations from intracellular stores, *J. Biol. Chem. 274*, 28682−28689.
26. Zhong, M., Yang, M., and Sanborn, B. M. (2003) Extracellular signal-regulated kinase 1/2 activation by myometrial oxytocin receptor involves $G\alpha_qG\beta\gamma$ and epidermal growth factor receptor tyrosine kinase activation, *Endocrinology 144*, 2947−2956.
27. Sealfon, S. C., Chi, L., Ebersole, B. J., Rodic, V., Zhang, D., Ballesteros, J. A., and Weinstein, H. (1995) Related contribution of specific helix 2 and 7 residues to conformational activation of the serotonin $5\text{-}HT_{2A}$ receptor, *J. Biol. Chem. 270*, 16683−16688.
28. Yang, M., Wang, W., Zhong, M., Philippi, A., Lichtarge, O., and Sanborn, B. M. (2002) Lysine 270 in the third intracellular domain of the oxytocin receptor is an important determinant for $G\alpha_q$ coupling specificity, *Mol. Endocrinol. 16*, 814−823.
29. Gether, U., and Kobilka, B. K. (1998) G protein-coupled receptors. II. Mechanism of agonist activation, *J. Biol. Chem. 273*, 17979−17982.
30. Menon, S. T., Han, M., and Sakmar, T. P. (2001) Rhodopsin: structural basis of molecular physiology, *Physiol. Rev. 81*, 1659−1688.
31. Raddatz, R., Crankshaw, C. L., Snider, R. M., and Krause, J. E. (1995) Similar rates of phosphatidylinositol hydrolysis following activation of wild-type and truncated rat neurokinin-1 receptors, *J. Neurochem. 64*, 1183−1191.
32. Namba, T., Sugimoto, Y., Negishi, M., Irie, A., Ushikubi, F., Kakizuka, A., Ito, S., Ichikawa, A., and Narumiya, S. (1993) Alternative splicing of C-terminal tail of prostaglandin E receptor subtype EP_3 determines G-protein specificity, *Nature 365*, 166−170.
33. Kwon, H. B., Oh, D. Y., and Seong, J. Y. (2003) Absence or presence of intracellular C-tail partly accounts for differential G protein coupling preference between mammalian and nonmammalian gonadotropin-releasing hormone receptors, *Biol. Reprod. 68* (Suppl. 1), 284 (abstract).
34. Ernst, O. P., Meyer, C. K., Marin, E. P., Henklein, P., Fu, W. Y., Sakmar, T. P., and Hofmann, K. P. (2000) Mutation of the fourth cytoplasmic loop of rhodopsin affects binding of transducin and peptides derived from the carboxyl-terminal sequences of transducin α and γ subunits, *J. Biol. Chem. 275*, 1937−1943.
35. Marin, E. P., Krishna, A. G., Zvyaga, T. A., Isele, J., Siebert, F., and Sakmar, T. P. (2000) The amino terminus of the fourth cytoplasmic loop of rhodopsin modulates rhodopsin-transducin interaction, *J. Biol. Chem. 275*, 1930−1936.
36. Cai, K., Klein-Seetharaman, J., Altenbach, C., Hubbell, W. L., and Khorana, H. G. (2001) Probing the dark state tertiary structure in the cytoplasmic domain of rhodopsin: proximities between amino acids deduced from spontaneous disulfide bond formation between cysteine pairs engineered in cytoplasmic loops 1, 3, and 4, *Biochemistry 40*, 12479−12485.
37. Yeagle, P. L., Choi, G., and Albert, A. D. (2001) Studies on the structure of the G-protein-coupled receptor rhodopsin including the putative G-protein binding site in unactivated and activated forms, *Biochemistry 40*, 11932−11937.
38. Krishna, A. G., Menon, S. T., Terry, T. J., and Sakmar, T. P. (2002) Evidence that helix 8 of rhodopsin acts as a membrane-dependent conformational switch, *Biochemistry 41*, 8298−8309.
39. Gimpl, G., Burger, K., Politowska, E., Ciarkowski, J., and Fahrenholz, F. (2000) Oxytocin receptors and cholesterol: interaction and regulation, *Exp. Physiol. 85* (Spec. No.), 41S−49S.
40. Guzzi, F., Zanchetta, D., Cassoni, P., Guzzi, V., Francolini, M., Parenti, M., and Chini, B. (2002) Localization of the human oxytocin receptor in caveolin-1 enriched domains turns the receptor-mediated inhibition of cell growth into a proliferative response, *Oncogene 21*, 1658−1667.
41. Crankshaw, D., Gaspar, V., and Pliska, V. (1990) Multiple [^{3}H]-oxytocin binding sites in rat myometrial plasma membranes, *J. Recept. Res. 10*, 269−285.
42. Baldwin, J. M., Schertler, G. F., and Unger, V. M. (1997) An α-carbon template for the transmembrane helices in the rhodopsin family of G-protein-coupled receptors, *J. Mol. Biol. 272*, 144−164.

BI035899M